



Clues to inferred different thrust-related fold models and thin-thick skinned tectonics within a single folded structure in Iraqi Zagros, Kurdistan region

Hassan Ghazi KakAmeen Balaki¹ · Abdulla Amir Omar¹

Received: 21 October 2017 / Accepted: 17 May 2018 / Published online: 13 June 2018
© Saudi Society for Geosciences 2018

Abstract

The Maqloub–BardaRash structure is situated at the Low Folded Zone within the NW of the Zagros fold-thrust belt in the Iraqi Kurdistan region. One of the main goals of this work is to reveal the variation in the fold architecture and fault shape with depth to build a plausible fold model, as well as to explain the kinematic evolution of the Maqloub–BardaRash structure. The middle part of the anticlinal hinge line of the studied structure shows deviation and anticlockwise rotation. This character is ascribed to the presence of a north-south trending left-lateral strike-slip fault. This fault is considered to be a deep-seated basement fault that likely caused segmentation of Maqloub–BardaRash structure into two parts: the northwestern Maqloub structure which exhibits a normal asymmetry and the southeastern BardaRash structure with a reverse asymmetry. The balanced cross sections based on the top of Middle Miocene Fatha Formation from the studied structures displays a maximum total horizontal shortening of 14% for the Maqloub structure and 9.89% for the BardaRash segment at the same stratigraphic level. Through the Maqloub section, the thrust-related shortening increases downsection, whereas the fold-related shortening increases upsection. Whereas along BardaRash section, the fold-related shortening smaller irregular variations at different stratigraphic levels are evidenced. The Maqloub segment is interpreted as a fault-propagation fold, but the BardaRash segment is interpreted as a faulted detachment fold based on the geometrical analysis of deformed models. Based on the resulting deformed geometries from the balanced cross sections, the propagation of the Maqloub segment is associated with the activation of an underlying basement fault, whereas the BardaRash segment is decoupled along the Triassic ductile sequence. The structural characterization of two different models of the fault-related deformation along the individual Maqloub–BardaRash folded structure will enhance accurate well position of the crestal reservoir.

Keywords Maqloub–BardaRash structure · Fault propagation fold · Faulted detachment folds · Balanced cross section · Thin skin · Thick skin

Introduction

The fault detachment fold model is closely analogous to the thrust propagation anticline, but it is a product of the transition in deformation pattern from detachment folding processes to progressive fault propagation folding (Mitra 2002; Mitra

2003). McClay (2004) presented a conceptual model based on Dobson (1991). This model exhibits three different fold deformation models that developed at same detachment level with progressive evolution. Here, during progressive evolution, with increasing fault displacement, the detachment fold changes to thrust propagation anticline, and ultimately to transported thrust propagation anticline.

The prolific oil and gas fields that were discovered within the Iraqi Kurdistan region in the previous years motivated several investigations (e.g., Kent 2010; Reif et al. 2011; Bretis et al. 2011; Csontos et al. 2012; Reif et al. 2012; English et al. 2015; Awdal et al. 2016; Koshnaw et al. 2016). Since tectonic deformation and propagation of the oil and gas bearing structures in the northwestern Zagros fold-thrust belt (ZFTB) segment in Iraqi Kurdistan are not well

✉ Hassan Ghazi KakAmeen Balaki
Hassan.Kakameen@su.edu.krd

Abdulla Amir Omar
Abdulla.omar@su.edu.krd

¹ Department of Geology, College of Science, Salahaddin University, Erbil, Kurdistan Region, Iraq

understood in comparison to the Iranian Zagros structures. Therefore, this study aims to (1) reveal the variation in the fold architecture and fault shape with depth to establish a plausible fold model, as well as to explain the fold kinematic evolution; (2) calculate the shortening ratio in two balanced cross sections across Maqloub–BardaRash structure; (3) deduce the deflection and rotation in the middle part of the hinge line of the studied structure; (4) decipher the abrupt rising of Maqloub segment with respect to BardaRash segment; and (5) infer tectonic style for studied structure.

The study area is located near the town of BardaRash, ~60 km northwest of Erbil, and bounded by longitudes $43^{\circ} 21' 40''$ and $43^{\circ} 45' 0''$ E and latitudes $36^{\circ} 25' 0''$ and $36^{\circ} 33' 20''$ N, within the Iraqi Kurdistan region (Fig. 1). The investigated area covers ~215 km² and is subdivided into two segments: Maqloub which is located to the NW of the studied area and BardaRash which occupies the SW portion of the studied area. Each of these segments has its distinctive morphotectonical, sedimentological, and structural character. The maximum elevation of the Maqloub and BardaRash segments are 1040 and 530 m above sea level, respectively. The

fold shape of the exposed part of Maqloub anticline created prominent topographic ridges in the area. This fold outline was well preserved in comparison to the fold shape of the adjoining synclines that form the broad valleys around Maqloub Mountain. These valleys are mostly occupied either by Pliocene rock beds or recent sediments.

Knowing the potential geometry of the fold type and fault shape with depth in addition to their evolution is crucial for the hydrocarbon exploration processes. Thereby, the accurate balanced sections are essential for selecting drilling locations and to identify structural traps with oil and gas accumulations (Mitra 1990; Mitra 1992; Poblet and Lisle 2013). The relationship between different models is great of importance as an indicator of type of reservoir. Mitra (2002) stated that the position and size of hydrocarbon reservoirs along the crest region of anticlinal fold are switched at transition from faulted detachment fold model to a fault propagation fold model. Accordingly, the position and size of oil traps through the crest area of studied major structure are altered during transition from BardaRash segment to Maqloub segment.

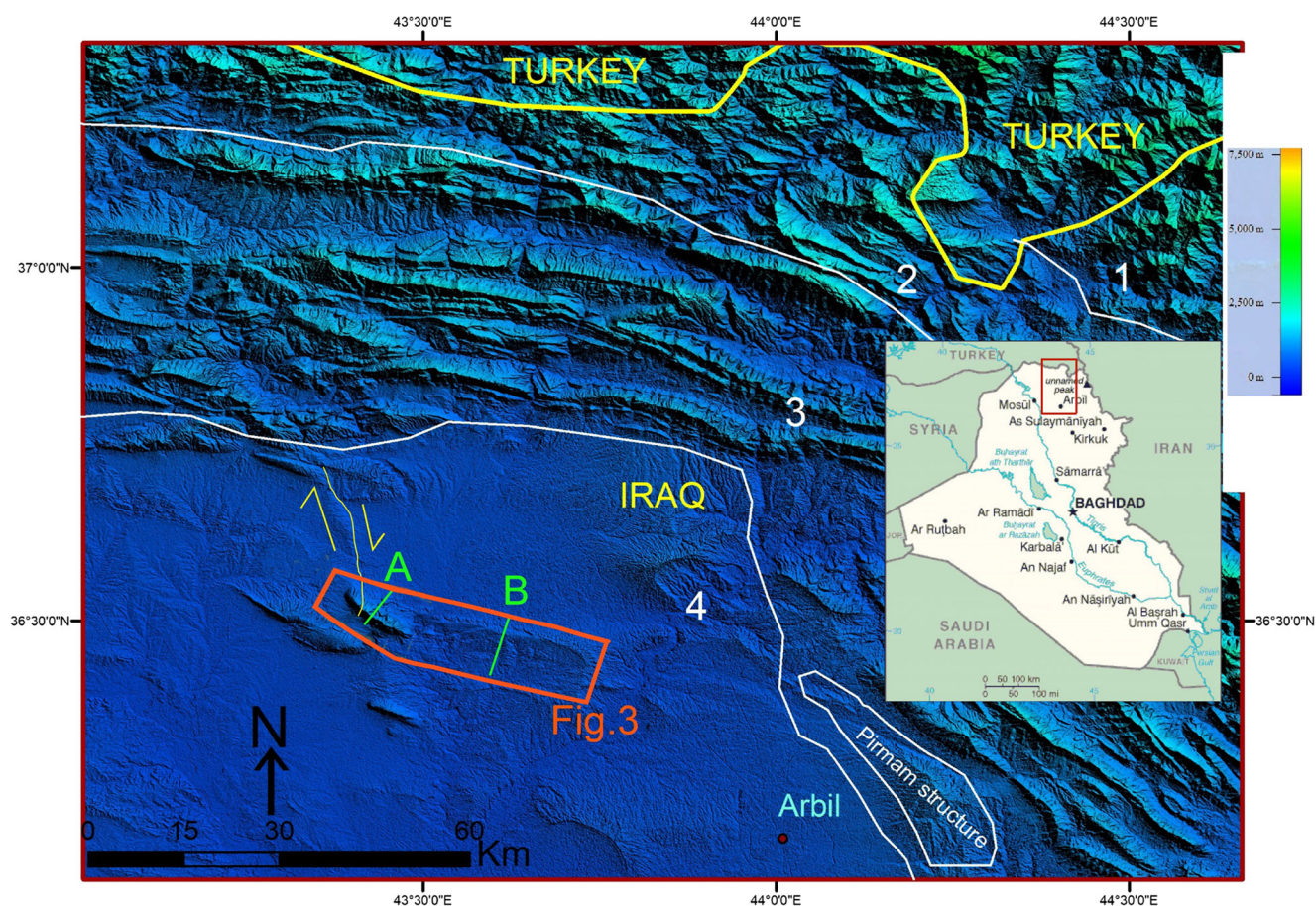


Fig. 1 Digital elevation model (DEM) of northern part of the Kurdistan Region of Iraq illustrating the location of the studied structure. Polygons enclose Fig. 3 with line of the sections A and B. Also, showing the tectonic subdivision of the NW Zagros Fold-Thrust Belt: (1) Zagros

Suture Zone, (2) Imbricate Zone, (3) High Folded Zone, and (4) Low Folded Zone. Additionally, illustrating the right-lateral strike fault affected on the northwestern part of Maqloub segment and fault persists toward north

Methods

The methods of the present work include obtaining field data and subsurface data and using them to construct detailed balanced cross sections and conduct structural analysis.

The fieldwork was conducted by following two traverses, perpendicular to the general trend of the hinge lines of anticline and synclines. The first traverse (A-A[−]) is 8 km in length and passing through the Maqloub segment. This traverse includes 27 field stations. The second traverse (B-B[−]) is 9 km in length and passes through the BardaRash segment. This traverse was covered by 29 field stations. The whole field investigation was achieved by 82 field stations. These stations were chosen on the basis of availability of well-exposed bedding surfaces, variation in dip panels through different structural positions (i.e., forelimb, backlimb, hinge regions of the fold), geological formation boundaries, and presence of the major fault traces. Furthermore, the fieldwork includes lithological description of the outcrop with determining lateral and vertical relationships between various strata of the Tertiary period. This succession included seven formations which are started by Paleocene-Eocene Kolosh Formation, and ended with Pliocene-Pleistocene Bai-Hassan (Upper Bakhtiari) Formation.

A few new available seismic reflection lines (that were close to selected sections) were integrated with the well data and field data to construct two balanced cross sections. To establish a two-dimensional geometrical model for the Maqloub–BardaRash structure, the geological surface data were projected with depth through their corresponding stratigraphic levels. The projection of the surface data with depth was constrained by the available seismic and well data, which they were penetrated sedimentary piles and reached the Triassic rocks.

Furthermore, hundreds of measured field data were projected and analyzed by employing equal area net to create fold elements that have strong relation with fold geometry. The geological cross sections were constructed manually, utilizing the kink method (Mitra 1992; Groshong 2006). In the studied area, most of the deformed sequences consist of stiff competent beds that conserve their orthogonal thickness and deformed primarily by flexural slip mechanism. The balanced cross sections were restored manually by removing the whole cumulative effects that arise from the deformation during folding and faulting processes. This implies retrodeformation of the strain ellipses into their corresponding unit circles via removing dip angles from the rotated layers (Howard 1993). In restoration and balancing processes of cross sections, two vertical pin lines were placed at the axial surfaces of two adjacent synclines, assuming that this region is a location of no inter-layer slip (Woodward et al. 1985; Woodward et al. 1989; Mitra and Namson 1989; Mitra 1992). In the next step, the bed length balancing started from the frontal vertical pin line rearward to hinterland vertical pin line; then, the line length

method was accomplished after several attempts to produce a plausible and feasible thrust fault geometry.

Geological setting

Tectonics

The Zagros orogenic belt is located along the northeastern margin of the Arabian Plate and constitutes a part of the extensive Alpine–Himalayan orogenic system. It formed during the progressive closure of the Neotethys Ocean due to the oblique collision between the Arabian and Eurasian plates (Golonka 2004; Agard et al. 2005). The closure of the Neotethys Ocean took place during Late Cretaceous–Cenozoic times (Talbot and Alavi 1996). The continental collision started in the Oligocene times and is active to present time (Fard et al. 2006). This continental collision led to folding and thrusting and emergence of the Zagros orogenic belt, as well as evolution of the foreland basin on the northwestern edge of the Arabian plate (Molinario et al. 2004; Fard et al. 2006).

Depending on the intensity of deformation and the structural geometry, the Zagros orogenic belt in Iraqi Kurdistan is subdivided into five zones that are structurally aligned in parallel to subparallel tectonic zones. These zones are divided by major thrusting boundaries from foreland (SW) to hinterland (NE) into (1) the Mesopotamian Foreland Basin, (2) Foothill Zone (FHZ) or Low Folded Zone (LFZ), (3) High Folded Zone (HFZ), (4) Imbricate Zone, and (5) the Zagros Suture Zone (Jassim and Goff 2006). The studied structure of this work, Maqloub–BardaRash structure, is a prominent faulted anticline situated within the LFZ (Fig. 1).

Stratigraphic framework

The sedimentary pile within the FHZ is consisting of competent sequences with relatively few weak incompetent beds, and total thickness of these mechanical anisotropy sequences ranges between 5 and 11 km with an average of 8–10 at NW block of the FHZ (Jassim and Goff 2006).

The Neogene sequence is exposed extensively across the FHZ; however, within few faulted anticlinal cores, the Paleocene beds are also observed (e.g., Maqloub anticline). In the following, the unexposed formations found in exploration well plus the exposed formations are described (Figs. 2 and 3). Starting from the Late Triassic rocks, Kurra Chine Formation consists of 850–1150 m of alternating thin and thick bedded limestone with intercalation of thick bedded dolomite and papery shale. In the subsurface section, thick evaporite intervals also exist within the formation, which has been deposited in intrashelf basins (Aqrabi et al. 2010).

The active deep-seated strike-slip faults are controlled deposition of the Phanerozoic piles at Zagros fold and thrust belt

Era	Period	Epoch/Age	Formations	Lithological symbols	Thickness (m)	Competency	Mega-sequences	Tectonic events			
Cenozoic	QUAT.	Holocene	Recent deposits		140-370	incompetent	AP 11	Late Zagros Orogeny, Folding and thrusting of Zagros Foreland			
		Pleistocene									
	Neogene	Pliocene	Bai-Hasan (U.Bakhtiari)		320-1760						
			Miocene	Mukdadiya (L.Bakhtiari)				470-1380			
		L	Injana (U.Fars)		320-370						
			M	Fatha(L.Fars)				160			
	Paleogene	Eocene	L	Pila Spi				310	competent	AP 10	Close of the Neo Tethys
			M	Gercus				50	incompetent		
			E	Sinjar-Kolosh				360	competent		
		Paleocene							incompetent		
							Inversion compression and ophiolite emplacement				
Mesozoic	Cretaceous	L	Maastrichtian	Shiranish		50	competent	AP 9	Post rift passive subsidence and extension		
			Campanian	Bekhme		90					
		E	Albian	U.Qamchuqa		150					
				U.Sarmord		60					
			Aptian	L.Qamchuqa		30					
			Barremian	L.Sarmord		110					
	Hauterivian	Garagu		70							
	Jurassic	L	Kimmeridgian				650	incompetent	AP 7	Break up of Gondwana	
				Oxfordian	Najmah						competent
		M	Callovian-Aalenian	Sargelu		210		incompetent			
Toarcian				Alan		130					
		Mus		40							
		Adaiyah		70							
E	Pliensbachian	Butmah		230	moderate						
Triassic	L	Rhaetian	Baluti		100	incompetent	AP 6	Opening of Neo Tethys			
		Norian	Kurra Chine			competent					
		Carnian				incompetent					

◀ **Fig. 2** Stratigraphic column of the studied structure illustrating the formation names, lithology, age, thickness, and competency based on the field and well data, with major tectonic megasequence (Sharland et al. 2001) and tectonic events (after Sissakian 2013)

(Hessami et al. 2001). Accordingly, the thickness variation of Late Triassic Kurra Chine Formation in particular evaporitic unit possibly occurs, where passing over present deep-seated strike-slip fault into Maqloub segment, thus changing from a ductile mobile detachment at BardaRash segment as crossing strike-slip fault to a frictional substrate throughout Maqloub segment (Cotton and Koyi 2000). The most upper part of Triassic rocks is represented by ~100 m of Rhaetic Baluti Formation. This rock unit composed of dominantly shale and bands of limestone and dolomite that deposited in lagoonal evaporitic and estuarine environments (Jassim and Goff 2006).

The Early Jurassic stratigraphy is defined by 470 m of carbonate-evaporite inner shelf succession, which are Butma, Adaiyah, Mus, and Alan Formations (Jassim and Goff 2006). The Middle Jurassic was defined by Sargelu Formation which is a thin bedded, bituminous, and dolomitic limestone containing black shales and streaks of thin black chert, and it was deposited in basinal euxinic marine environment (Jassim and Goff 2006). Sargelu Formation thickness is about 200 m in subsurface section. The Late Jurassic is topped by neritic oolitic limestone and lagoonal facies of Najmah Formation which attain its largest thickness (443 m) in well Demir Dagh-1 close to the studied Maqloub–BardaRash structure (Sadooni 1997).

The Early Cretaceous Garagu Formation (~70 m thick) is constituted mainly from coarse-grained oolitic limestone with some ferruginous sandstone rocks that deposited in a high-energy and shallow water environment (Aqrabi et al. 2010). The Garagu Formation was capped by 140 m of Lower Sarmord Formation and Lower Qamchuqa Formation. The Lower Sarmord Formation (110 m thick) comprises marl, with beds of argillaceous limestone. The formation was deposited in a deep inner-shelf to outer-shelf environment (Jassim and Goff 2006). The Lower Qamchuqa Formation consists of (30 m thick) of thick bedded carbonate rocks which represent deep-ocean facies. The Albian carbonate ramp was represented by 210 m of the Upper Sarmord (marl and limestone) and the Upper Qamchuqa Formations (carbonate). The Upper Sarmord Formation was deposited in inner-shelf lagoons, whereas Upper Qamchuqa Formation represents shallow inner-shelf environment (Jassim and Goff 2006). The Late Cretaceous is defined by two formations. The first is Bekhme Formation, which consists of 90 m of reefal limestone and fore-reef limestone. The Bekhme Formation unconformably underlies by Upper Qamchuqa Formation (Bellen et al. 1959). The second formation is the Shiranish Formation (50 m thick) that composed of pelagic marl underlain by well-bedded limestone (Bellen et al. 1959).

The oldest exposed rocks (Paleocene-Early Eocene) in the eroded core of the Maqloub anticline is the clastics of flysch deposits of Kolosh Formation (360 m thick), which is interfingering with lagoonal carbonates of the Khurmala Formation (Bellen et al. 1959). The Middle Eocene rock is represented by ~50 m of red clastics of molasses (Gercus Formation), which was capped by ~310 m of lagoonal limestone of Pila Spi Formation (Middle-Late Eocene). The Pila Spi Formation consists of competent rock units that are resistant to erosion and weathering in comparison to the overlying and underlying formations. Therefore, it forms the carapace of the Maqloub anticline. The Middle Miocene Fatha (Lower Fars) Formation unconformably overlies the Middle-Late Eocene Pila Spi Formation. The exposed Fatha Formation in the study area includes ~160 m of gypsum interbedded with fossiliferous limestone, marly limestone, and marl. The Fatha Formation represents a rapidly subsiding sag basin which occasionally altered to evaporitic environment (Jassim and Goff 2006). The Late Miocene Injana (Upper Fars) Formation has been recognized by the first occurrence of sandstone, and it constitutes of (320–370 m thick) repetitive interbedded resistant sandstone beds separated by easily erodible mudstones. Thereby, the lower boundary of Injana (Upper Fars) Formation with the Fatha Formation is gradational. Also, the upper boundary with the Late Miocene Mukdadiya (Lower Bakhtiari) Formation is gradational indicated by occurrence of gravely sandstone (Jassim and Goff 2006). The Late Miocene Injana (Upper Fars) Formation composed of synorogenic sediments that was produced by the erosion of the uplifted Zagros Mountain belt during a collision (Pirouz et al. 2011). The Late Miocene Mukdadiya (Lower Bakhtiari) Formation consists of 470–1380 m of mudstone and intercalated by sandstone and pebbly sandstone. The sandstone was characterized by coarse- to very coarse-grained, poorly cemented, and bluish gray in weathered color. The Mukdadiya Formation represents fluvial deposits of a rapidly subsiding foredeep basin (Jassim and Goff 2006). The Pliocene-Pleistocene Bai-Hassan (Upper Bakhtiari) Formation is regarded to be the youngest synorogenic sediments of the Zagros foreland basin. It consists chiefly of very thick to massive conglomeratic beds with cross-bedded gravels, sandstones, and claystone. The Bai-Hassan Formation reflects alluvial fan deposits originated from the Zagros suture and High Folded Zone (Jassim and Goff 2006).

Structural analyses

In order to obtain a three-dimensional structural analysis for the studied structure, this section is subdivided into the plan view and cross-sectional view description, and the geometrical analysis.

Plan view description

The Maqloub–BardaRash is bounded from the southeast by the Dusara syncline, and Merge syncline and from the northeast through the Gr kal-Amyan syncline. The deformed sequence that exposes at this major structure ranges from the Paleocene-Early Eocene Kolosh Formation to the Pliocene-Pleistocene Bai-Hassan (Upper Bakhtiari) Formation. The Pila Spi and Upper Fars Formations outcrops compose most of the crestal domains and surrounding area of the hinge at the Maqloub and BardaRash segments. The entire Maqloub–BardaRash structure is 35 km long and 4 to 2.5 km wide with a maximum elevation of up to 1040 m in the middle part of the Maqloub segment. The Maqloub–BardaRash structure extends from Taq Hama village at the northwestern plunge to Biyuk village at SE plunge (Fig. 3). The overall geometry of the Maqloub segment is an arcuate outward convex shape that can be observed from satellite images (Fig. 1). In general, the anticlinal hinge line along the Maqloub segment is trending 303°–123°, but deflecting to 282°–102° at the BardaRash segment. Thus, the difference between hinge line trend in both segments approaches 20°.

The Maqloub segment is affected by three emerging major thrust faults that dip between 72° and 78°, either foreland (SW) verging or hinterland (NE) verging and dip slip displacement partitioned among them. These thrusts, from the northeast toward the southwest, were labeled first Maqloub thrust (MT1), second Maqloub thrust (MT2), and third Maqloub thrust (MT3) (Fig. 3). The MT1 is back thrust with hinterland (NE) verging, whereas MT2 and MT3 are forelimb imbricate thrusts with foreland (SW) verging. The maximum dip slip displacement is observed across (MT3) through which the forelimb of the anticline is cut by MT3 and leading to transport the entire anticline toward foreland on the top of a gently dipping beds in the footwall. In other words, the lower part of the Fatha (Lower Fars) Formation (Middle Miocene) in the forelimb of the Maqloub segment overrides the upper part of Injana Formation (Late Miocene) in the trough of the Merge syncline, with an estimated stratigraphic separation of 250–300 m (Figs. 3 and 4). Here, in the vicinity of the fault surface MT3 within the evaporite strata of Fatha (Lower Fars) Formation, slicken side striations were detected. These striations exhibit two different orientations. These striations probably developed either as a result of rotation of the bedding plane with respect to the stress field or rotation (i.e., change

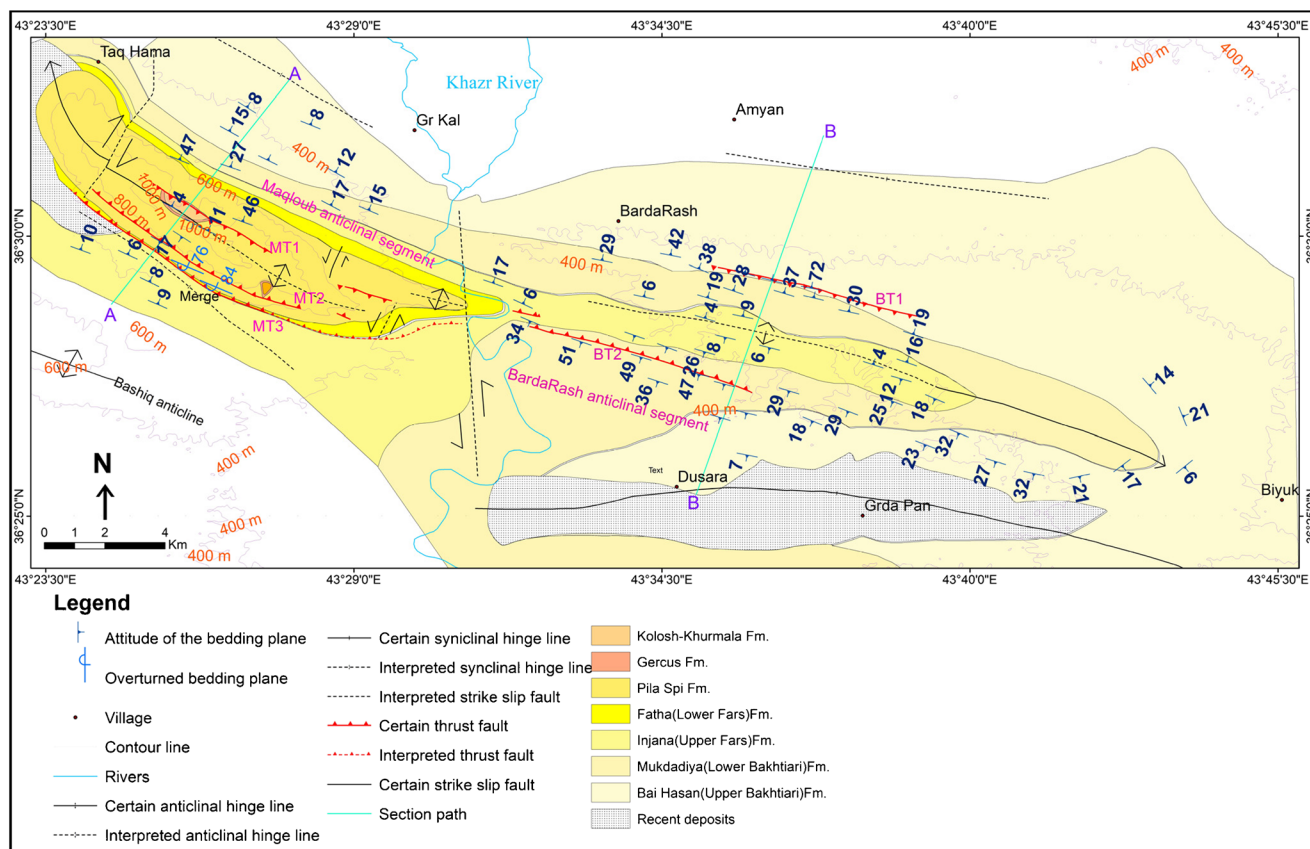
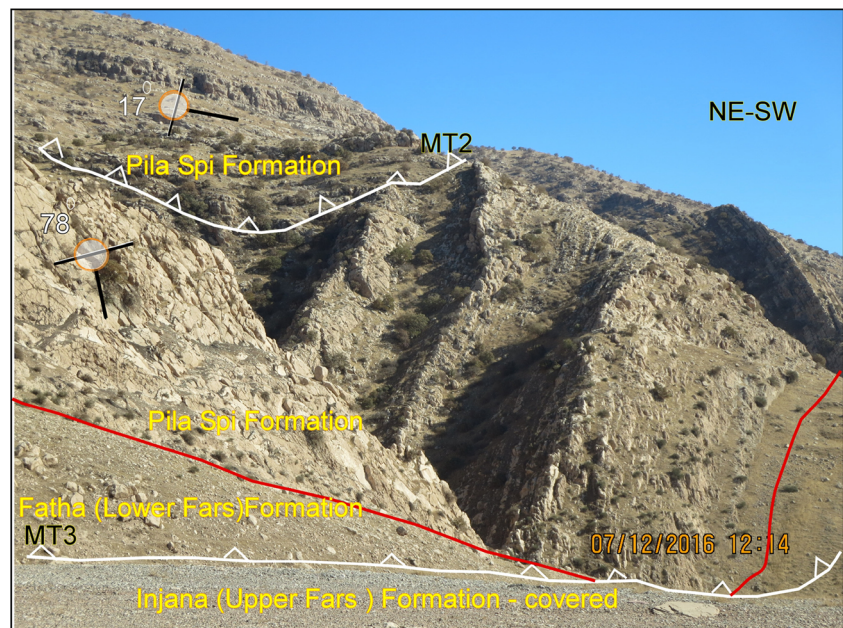


Fig. 3 Geological map of the Maqloub–BardaRash structure. This structure exhibits the Cenozoic formations that divided by a major strike-slip fault into two segments: the western Maqloub segment and the eastern BardaRash segment

Fig. 4 Field view of the southwestern forelimb of Maqloub segment showing the two major thrusts MT2 and MT3, which are bounded subvertical beds of the Middle-Late Eocene Pila Spi Formation



in orientation) of the stress field with respect to the bedding plane. The existence of more than one set of striations or curved slickenside striation is resulted from more than one generation of movement. MT1 broke through the backlimb of the Maqloub structure, and placed the Paleocene-Early Eocene Kolosh Formation over the Middle Eocene Gercus Formation (Fig. 3). In contrast, the MT2 broke through the southwestern flank of the Maqloub segment, where Middle-Late Eocene Pila Spi Formation overrides itself across MT2 (Figs. 3, 4, 5a, b, 6, and 7).

Toward the extreme northwest and southeast along the MT1 and MT2, the displacement declines to its minimum value, where the Pila Spi Formation overrides itself. At this fault, the whole fault dip slip of MT1 and MT2 is transferred progressively to the Maqloub anticline on its high-angle thrust ramp tip. This fault behavior gives an impression that the thrust-related anticline is reflecting a fault propagation folding processes that will be discussed later.

Along the middle parts and the periphery of the Maqloub segment, the distribution pattern of the geological boundaries reflects existence of a major double-plunging asymmetrical anticline. The southwestern forelimb of the Maqloub anticline is shorter (narrower) and steeper (partly overturned in places) than their corresponding backlimb. In general, on the forelimb, the dip panels of beds rapidly vary toward the southwest. It steepens to nearly vertical and then becomes overturned between MT2 and MT3. Rock beds exposed on the forelimb are Pila Spi Formation and lower part of the Fatha (Lower Fars) Formation. These subvertical to overturned beds of the Pila Spi Formation, which bounded between two adjacent major thrusts (MT2 and MT3), indicate that these two thrusts evolved along the preexisting axial surfaces bounding a dip

panels within the forelimb. Accordingly, formerly developed axial planes are reasonable sites for generating thrust planes. Also, the field investigations support this consideration via existence of some smaller thrusts with dip displacement of 4–6 m in the vicinity to the axial surfaces that separated dip panels. Such type of secondary thrust faults are considered as fold-accommodation thrusts and most probably developed during progressive tightening of the fold (Fig. 8).

The entire northeastern backlimb plus parts of the hinge zone of the adjacent Merge syncline were buried beneath the Maqloub thrust faults. Rock units exposed on the southwestern forelimb of Merge footwall syncline are Injana (Upper Fars) and Fatha (Lower Fars) Formations, and the dips of strata increase from 6° NE close to the hinge zone to around 25° NE at the inflection line.

The hinge zone of the Maqloub anticline is broad and segmented into dip panels. The hinge region is limited by traces of MT1 and MT2. The hinge area becomes broader toward the northwestern and the southeastern plunges owing to reduction in thrust displacement values along imbricated thrust faults (MT1, MT2, and MT3), as well as a decrease in steepness of forelimb. This variation in the Maqloub anticline geometry along its strike reflects variations through time (Fig. 9).

The northeastern limb of the Maqloub anticline occupies most of the area limited by MT1 or the hinge trace of the Maqloub anticline and rearward to the northeast inflection line with adjoining Gr-Kal footwall syncline. The exposed sequences across the backlimb are Gercus and Pila Spi Formations. The rock beds on this limb are dipping toward NE, and the dip angle increases from 4° at the hinge zone to ~46° close to the inflection line. The inflection line between the backlimb of the Maqloub anticline and the southwestern

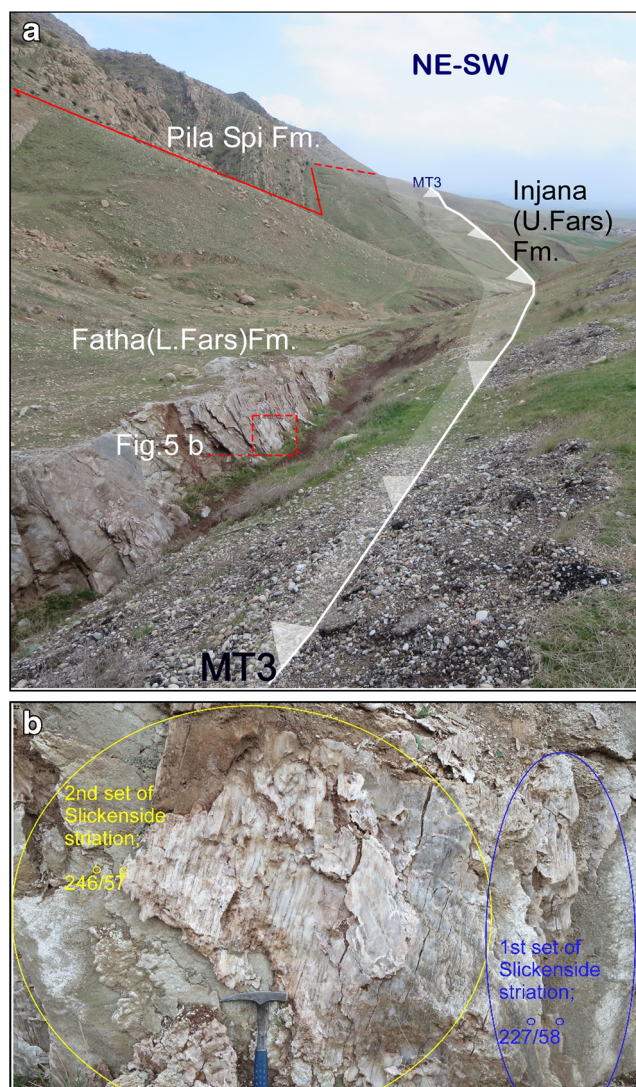


Fig. 5 **a** The photograph illustrating location (red rectangle) of the slickenside striations that were detected in the vicinity to the fault surface MT3 within the evaporite strata of the Middle Miocene Fatha (Lower Fars) Formation. **b** Two different orientation of striations which marked by different color

limb of the Gr-Kal syncline passes roughly along the top of Pila Spi Formation (Fig. 3).

The Maqloub thrust-related fold is cross cut by two distinct map scale strike-slip faults. The first strike-slip fault affects the Maqloub structure at the northwestern plunge and it continues toward the north (Fig. 1). This right-lateral strike-slip fault is oblique to hinge line of Maqloub anticline and caused rotation and/or shifting of the hinge line. The measured horizontal displacement on it is ~140 m. The second strike-slip fault oriented NE-SW with a shorter trace affected the Maqloub structure near to the southeastern plunge of Pila Spi Formation. This strike-slip fault has left-lateral movement and led to abrupt bending of the Pila Spi–Fatha Formation boundary with horizontal displacement estimated by ~350 m (Fig. 3).

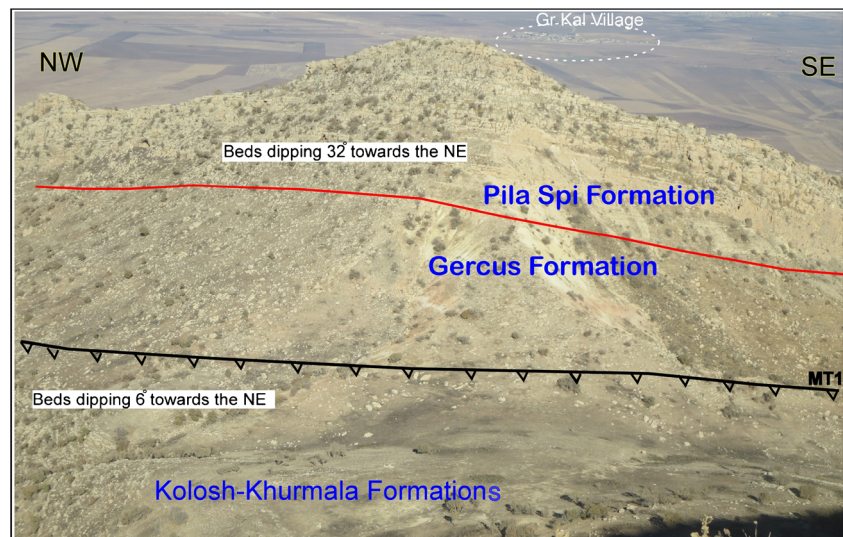
The BardaRash segment is affected by two major oppositely directed thrust faults. These emerging thrust ramps dipping of 64° – 68° , based on calculations from seismic profile. These thrusts from the northeast toward the southwest are first BardaRash thrust (BT1) southwest dipping and NE verging, while second BardaRash thrust (BT2) is SW verging. The frontal thrust BT2 broke through the forelimb of BardaRash anticline and placed the lower part of Late Miocene Mukdadiya Formation over the middle part of same formation (Fig. 3). The back thrust BT1 broke through the backlimb of the BardaRash segment and brought the lower part of the Pliocene–Pleistocene Bai Hassan over the upper parts of the same Formation with a stratigraphic separation that ranges between 650 and 750 m (Fig. 10).

The southwestern limb of the BardaRash segment consists of most of the area bounded by the hinge trace and inflection line between this forelimb and Dusara footwall syncline. The inflection line passes approximately along the upper parts of the Mukdadiya (Lower Bakhtiari) Formation. The outcropped rock units across the forelimb are Late Miocene Injana (Upper Fars) and Mukdadiya Formations. The rock strata are dipping toward SW, and the angle of dip increases from $\sim 8^{\circ}$ SW at the hinge region to $\sim 38^{\circ}$ SW close to the inflection line. Thus, the southwestern limb demonstrates four dip domains, which from hinge area to inflection line are dip angles of 8° (Injana Formation), 16° (Injana–Mukdadiya Formation boundary), 29° , and 47° (Mukdadiya Formation). On the other hand, the northeastern backlimb divided into five dip panels that from higher level to lower level correspond to 6° (Injana Formation), 19° (Injana–Mukdadiya Formation boundary), 28° , 37° (Mukdadiya Formation), and 54° (Bai-Hassan Formation). The anticlinal crest was recognized with an ~1000-m-wide smoothly rounded surface. Such characteristic was interpreted as fault detachment fold that will be discussed later. In the cross-section profile, this wide crestal region has been divided into four dip domains (Figs. 11 and 13).

Geometry at depth the Maqloub–BardaRash anticline

Two structural balanced and restored cross sections were constructed across the Maqloub–BardaRash anticline. The cross section across the Maqloub anticline extends from the surface to the Pre-Cambrian basement, whereas the cross section across the BardaRash anticline reaches the Upper Triassic Kurra Chine Formation (Fig. 13). In both sections, the study area includes the Maqloub–BardaRash thrust anticline and their adjacent footwall synclines. The hinge lines of the both Maqloub and BardaRash segments are trending NW-SE, and their axial surfaces are dipping at a high angle either toward NE as in the Maqloub part or directed to SW as in the BardaRash segment. In the Maqloub segment, the hinge zone is broad and the interlimb angle is $\sim 100^{\circ}$ and gradually increases toward the plunges to $\sim 120^{\circ}$, where the hinge zone is

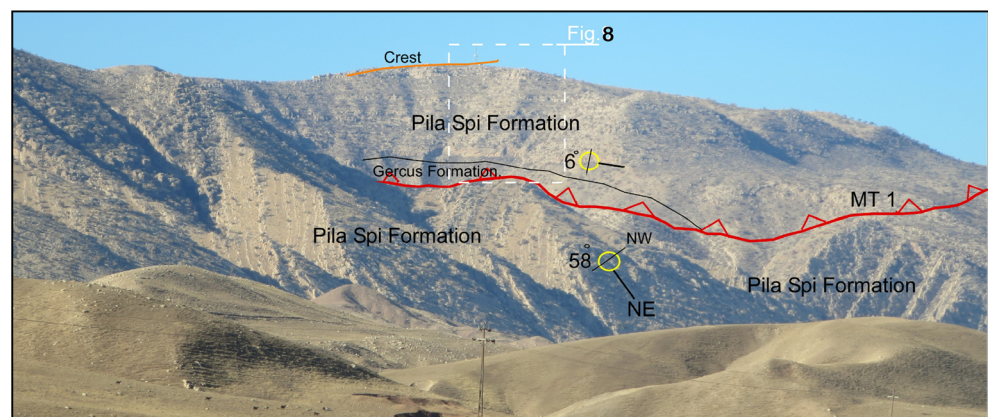
Fig. 6 Aerial field view showing the northeastern backlimb of the Maqloub segment which is breaking through by a back thrust and led to climbing of the middle parts of the Kolosh-Khurmala Formation on the Gercus Formation



broadening relatively. The overturned beds were observed in the Maqloub hanging wall anticline toward the southeast of section A-A⁻, particularly between MT2 and MT3, which might be rotated to overturning during the late stage movement on the MT2 and MT3, and thereby, these rotated beds continue to reasonable depths. These overturned beds are considered to represent the further shortening within the Maqloub segment as consequence of the dip angle increasing on the frontlimb (Mitra 1990; Jabbour et al. 2012) (Fig. 12).

The cross-sectional geometry of the BardaRash segment indicates existence of a major hanging wall thrust anticline with a pop-up structure that developed upsection between BT1 and BT2. It appears that the back thrust cut up from the associated forethrust and led to the development of the pop-up structure. The BardaRash segment has rounded to sub-rounded hinge zone with relatively curved limbs. The fold amplitude and fold aspect ratio of the Maqloub segment that measured from the balanced section A-A⁻ (Fig. 12) at the top of Pila Spi Formation are ~710 m and 0.26, respectively. Whereas, the fold amplitude and fold aspect ratio of the BardaRash segment that were calculated from the section B-B⁻ (Fig. 13) at the top of the same stratigraphic level are ~590 m and 0.19, respectively.

Fig. 7 View showing crest area and the northeastern backlimb of the Maqloub segment. The NE flank is breaking through by the back thrust MT1. The Pila Spi Formation, which forms the carapace of this anticline, can be observed forming the NE flank at the lower part of the photograph



Along part of the back thrust BT1 in the BardaRash anticline, the complicated variations in the fault slip resulted in nonuniform variations in dip displacements within Jurassic and Upper Triassic formations. While, along MT1 and MT2 (Fig. 12) in the Maqloub segment, the fault slip pattern demonstrates a uniform variation and the displacement decreases progressively upsection. For instance, updip, the displacement decreases from ~500 to ~60 m along the MT2. The reduction in the thrust dip displacement updip (i.e., decrease in the fault-related shortening) is balanced by an increase in the fold-related shortening (Mitra 1986; Pennock et al. 1989). The decrease of the displacement upsection provides a mechanism by which thrust can lose displacement upward. In this mechanism, the major fault ramp loses displacement by bifurcating into numerous smaller and minor splays and distributing its displacement among them (Dahlstrom 1969; Mitra 1986). In the section B-B⁻, there is a thickening in the Upper Triassic Kurra Chine Formation in the core of the anticline. This may be owing to the existence of thick incompetent units possibly containing evaporites and shale (Fig. 13).

The thickness variation of the Mukdadiya Formation was detected along both flanks of the BardaRash segment

Fig. 8 Crest area of the Maqloub segment illustrating smaller thrusts that are growing in the vicinity to the axial surfaces. These small thrusts separated the dip panels and bifurcated into minor faults from thrust fault

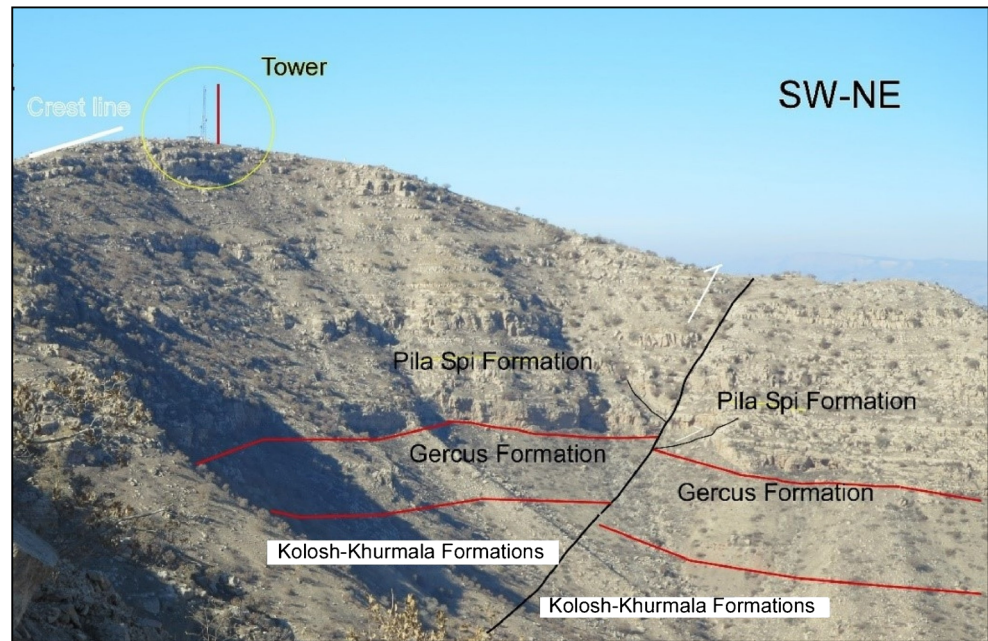


(Fig. 13). Shaw et al. (2005) point to that the thickness variations of the synorogenic growth units are constrained principally by the deformation kinematics and relative rates of the sedimentation and uplift. So that, where sedimentation rate exceeds uplift rate, the syntectonic growth bed thins onto the structural high (anticlinal crest) (Shaw et al. 2005). Consequently, the thickness change of the Mukdadiya Formation along both limbs within footwalls of BardaRash thrust structure is probably ascribed to the differential sedimentation rate and uplifting rate across both sides of major structure. On the other hand, syntectonic growth assemblages have been employed for knowing time of deformation in many compressive settings (Masferro et al. 2002; Horton et al. 2002; Sun and Zhang 2009; Koshnaw et al. 2016). In the current work, the thickness variation of the Mukdadiya Formation across both limbs of the BardaRash segment likely indicates that this segment was active during deposition of the Late Miocene Mukdadiya Formation.

Cross-sectional geometry A-A⁻ and B-B⁻ (Figs. 12 and 13) reveal that the southwestern frontal synclines are higher than the northeastern synclines. This abnormal structural feature is possibly ascribed to existence of the underlying thrust

fault that rooted either within Phanerozoic stratigraphic succession or Precambrian basement.

Geometrical analyses

Depiction of fold geometry is an important aspect in this study as it permits us to do geometrical comparison between the two segments of the major structure.

Maqloub segment was analyzed geometrically through section A-A⁻. The stereographic projection of the bedding plane within the different stratigraphic formations shows three separated pole clusters, representing three main dip domains across the backlimb. The mean attitude of front and backlimbs are 213°/44° and 023°/34°, respectively, which indicate the existence of a normal asymmetrical anticline with a greater dip value in the forelimb. The hinge line plunges 4° toward 299°, while the hinge surface is dipping 85° toward 028°. Consequently, the vergency of the Maqloub segment is toward the southwest (foreland). The folding angle and interlimb angle values are 79° and 101°, respectively; therefore, the Maqloub anticline represents an open fold and upright subhorizontal fold as well (Fig. 14).

Fig. 9 Photograph illustrating the decrease in steepness of the Maqloub segment toward SE plunge. In this photo, Kink band geometry well recognized with their dip panels separated by axial surfaces

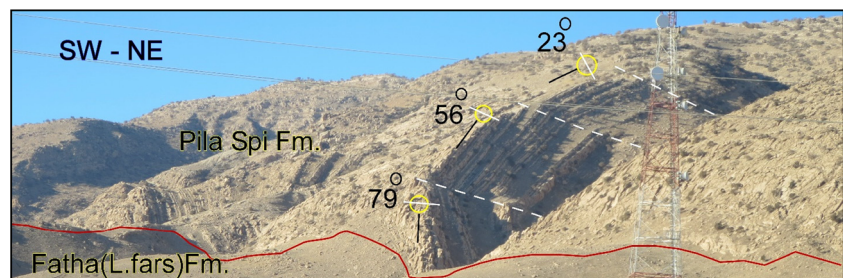
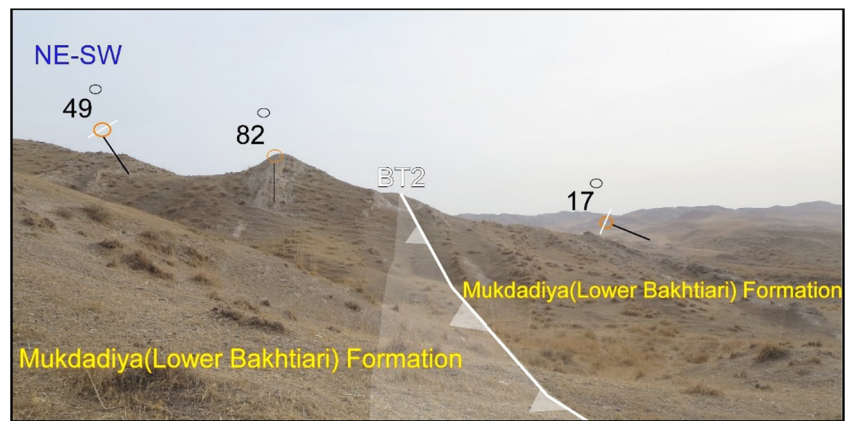


Fig. 10 Photograph illustrating thrust fault BT2 with southwestern vergency breached the southwestern forelimb of the BardaRash segment. This thrust was brought older units of the Late Miocene Mukdadiya Formation over younger parts formation itself



The synoptic stereographic representation of strata at different stratigraphic units from the BardaRash segment reveals different structural characteristics. The average orientation of the front and backlimbs are $197^{\circ}/25^{\circ}$ and $015^{\circ}/31^{\circ}$, respectively, which point to presence of a reverse asymmetrical anticline with a greater dip amount at the backlimb. The orientation of hinge line and hinge surface are $286^{\circ}/1^{\circ}$ and $196^{\circ}/83^{\circ}$, respectively. This indicates a discrepancy in the vergency between the BardaRash segment that directed toward northeast (hinterland) and the Maqloub segment. Also, folding angle and interlimb angle exhibit different values which are 56° and 124° , respectively. Hence, the BardaRash segment represents an open to gentle fold with a curvilinear axial surface (Fig. 15).

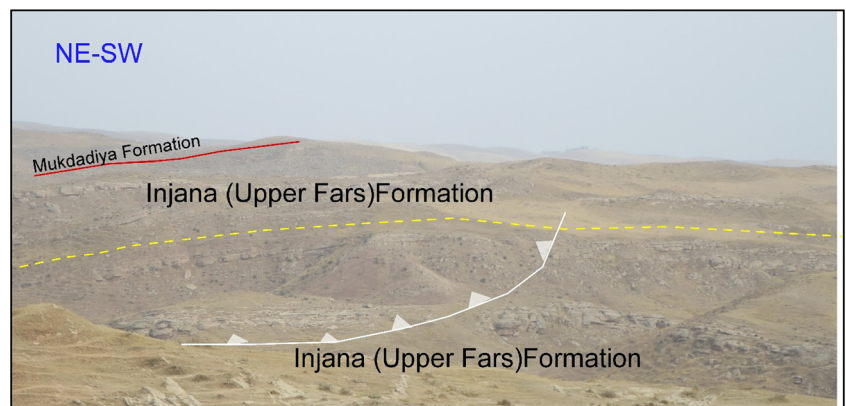
Discussion

Calculation of shortening in different time and space

The total horizontal shortening is the sum of shortening resulted from displacement on the major thrusts and folding processes as well as the shorting produced from the internal deformations. In the current study, the internal deformations are very rare and negligible in comparison to the folding and thrusting processes.

The balanced cross sections exhibit vertical variation, as well as, along strike variation in the values of shortening at the different stratigraphic levels. The details of these variations in both sections were measured and recorded in Table 1. In general, section A-A⁻ (Fig. 12) shows that shortening due to faulting increases downsection. The increasing of the shortening due to thrusting is directly related to the dip angle in addition to displacement value along the thrust surface. The dip angles exhibited little variation in their values within different stratigraphic levels based on a proprietary seismic profile. Therefore, this increase in shortening due to thrusting is primarily ascribed to progressive increment in the displacement values downsection. Thus, the minimum amount of shortening due to thrusting was calculated at the top of the Gercus Formation (Middle Eocene) and indicated 138 m. The greatest amount of shortening due to faulting is 346 m and was measured at the top of the top Alan Formation (Early Jurassic). In contrast, the largest amount of shortening was due to folding calculated upsection at the top of the Fatha Formation (Middle Miocene) and indicated 834 m. This value is related to relatively high folding amplitude within this stratigraphic horizon. The lowest amount of shortening measured downsection is estimated by 294 m, which is measured at the top of the Alan Formation (Early Jurassic). This low value of shortening is ascribed to low amplitude and long wavelength of the fold

Fig. 11 Field view showing the wide anticlinal crest area of the BardaRash structure. The Late Miocene Injana (Upper Fars) Formation occupies the hinge area of this anticline. The smaller scale thrust fault with displacement ~30 m developed at crestal area which caused discontinuity in crestal dip domain



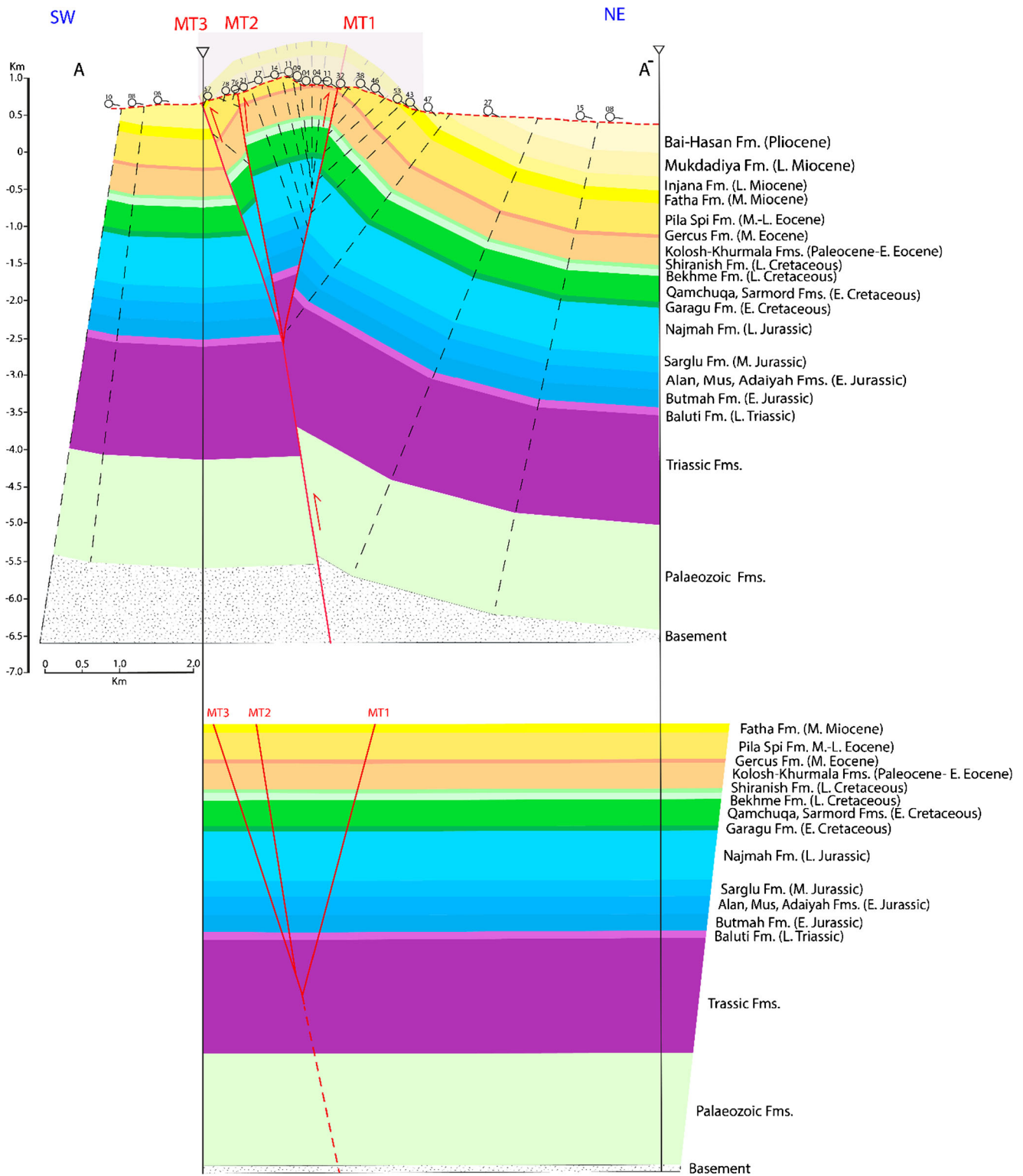


Fig. 12 Balanced cross section and its restored counterpart for the Maqloub segment through section line A-A⁻

within this stratigraphic level. At section A-A⁻, it seems that the intensity of folding and thrusting reach to their maximum magnitude along the studied structure. The greatest displacement observed is in the middle part of the Maqloub segment, which denote to the thrust fault nucleation region (e.g., Ellis

and Dunlap 1988; McConnel et al. 1997; Tavani et al. 2006). Thereby, the Maqloub anticline hanging wall generated as open anticline and became tighter with incremental displacement as observed in the central parts of the anticline (Table 1).

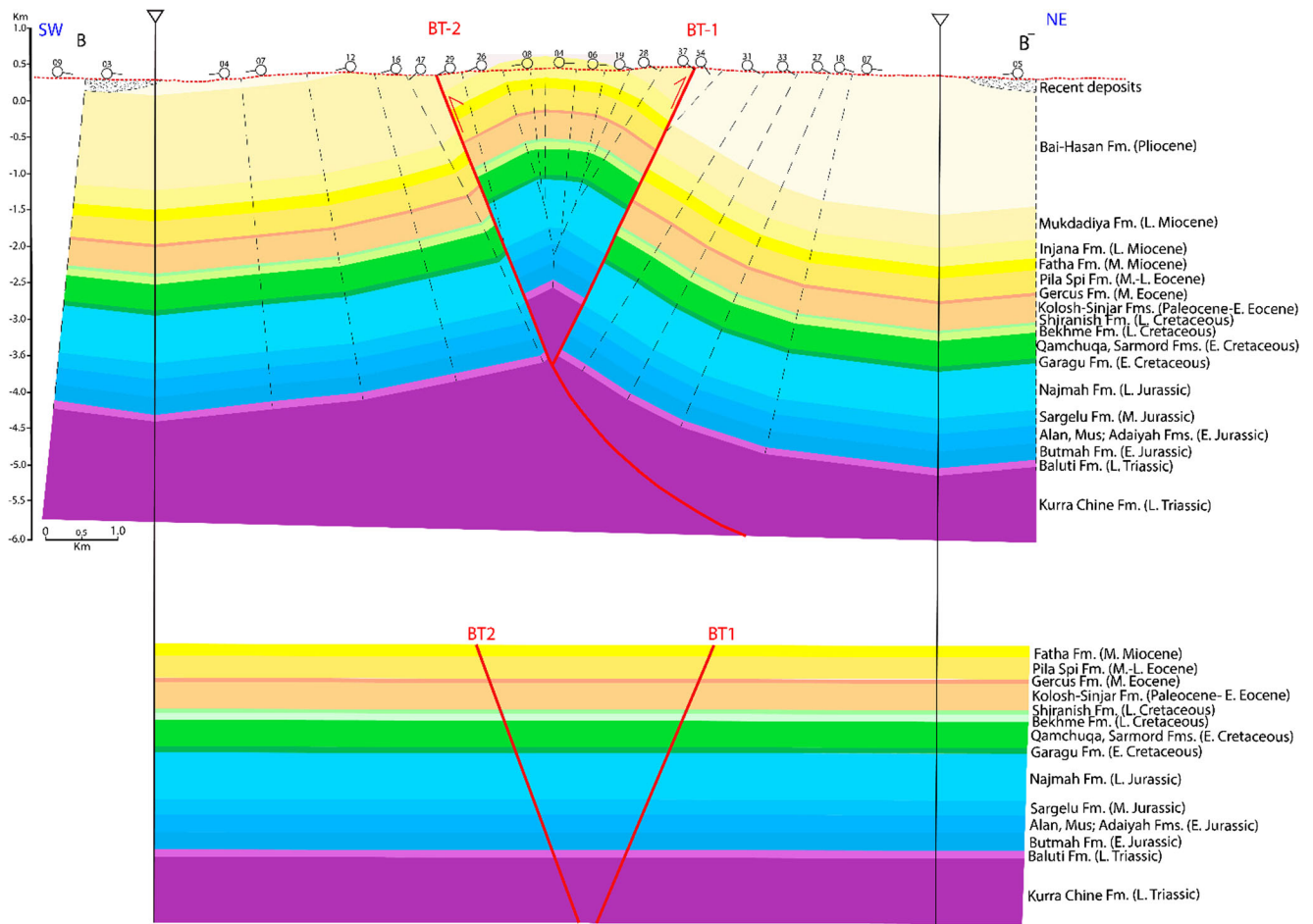


Fig. 13 Balanced and restored cross sections of the BardaRash segment through section B-B⁻

The section B-B⁻ (Fig. 13; Table 1) displays smaller vertical variations in the magnitude of shortening that related to thrusting in comparison to the section A-A⁻ (Fig. 12). Such smaller values are possibly due to the lesser variations in dip slip displacement along the thrusts within the different stratigraphic levels. Also, the section B-B⁻ (Table 1) is exhibiting smaller vertical variations in the amount of shortening due to folding in comparison to the section A-A⁻; this is mainly due

to lesser vertical variations in the wavelength and the amplitude ratio within the various folded stratigraphic units. In other words, these smaller vertical variations in the wavelength and amplitude ratio are reflecting small variation in the anticlinal length. Such difference in the BardaRash and Maqloub segments reflects variation in their models of fold evolution. The current results of shortening are in agreement with other estimations of shortening across the ZFTB that estimated to be

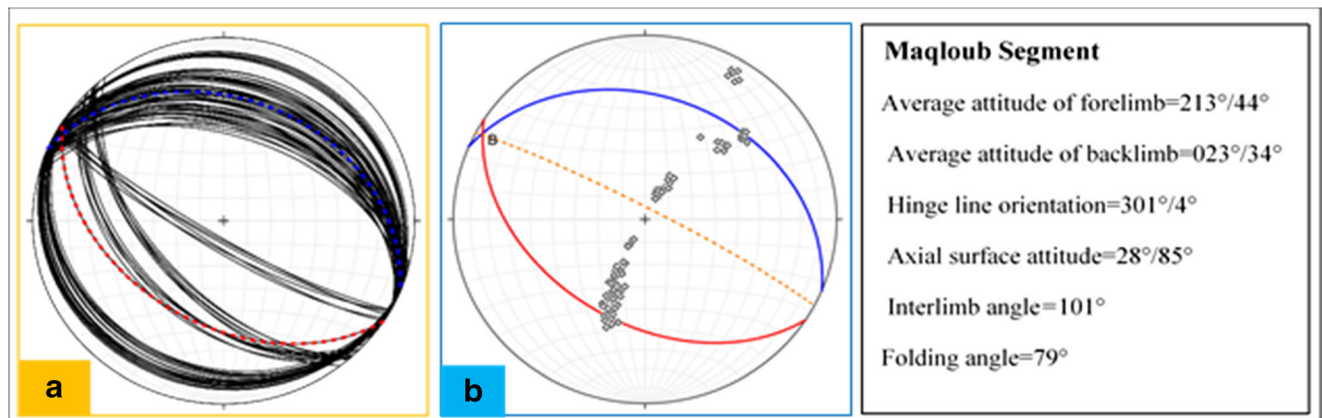


Fig. 14 Stereographic projection representing beta diagram (a) and Pi diagram (b) of the Maqloub segment

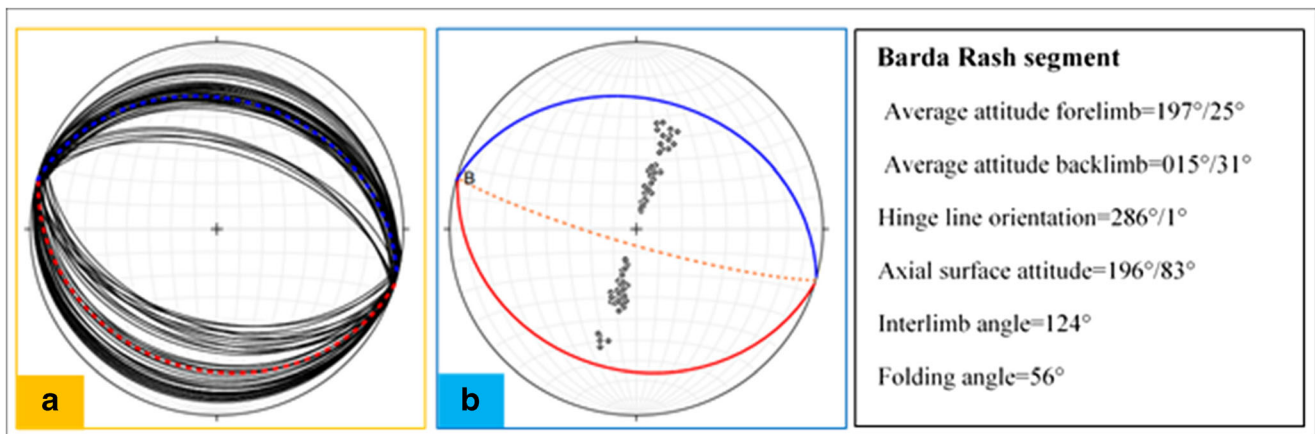


Fig. 15 Stereographic projection representing beta diagram (a) and Pi diagram (b) of the BardaRash structure

ranged 10–15% (McQuarrie 2004; Emami et al. 2010; Verges et al. 2011; Frehner et al. 2012; Omar and Syan 2016; Koshnaw et al. 2016). These measurements are estimated by using structural balanced cross sections either across an anticline or more than one structures.

Strike-slip fault

As mentioned in the previous section, the difference in the hinge line trend between Maqloub segment and BardaRash segment is about 20°. The deflection and anticlockwise rotation were prompted by a major left-lateral strike-slip fault that trends north-south oblique to the major structural hinge line. Burberry (2015) has suggested that the strike-slip fault could be a deep-seated fault, associated with the activation of an underlying basement fault underneath the studied structure. Also, the same strike-slip fault possibly caused translation of strain from foreland at Maqloub segment, and toward hinterland at the BardaRash segment. Maleki (2015) studied a structure at the SE Zagros of Iran, and obtained similar results with regard to the translation strain from foreland toward hinterland. Depending on the fault trend, the strike-slip fault may belong to the Nabatah transpressional fault system, which is recognized as oldest fault system within the Arabian plate that evolved during the Nabatah orogeny 680–640 Ma (Quick 1991; Burberry 2015). This basement fault is passing through the middle part of Maqloub–BardaRash structure nearby Khazr River, and this fault shows continuity at both ends (Fig. 3).

The present basement strike-slip fault has a great impact to the cover shortening. Thus, interaction between traces of the basement fault and thrusts in the Maqloub–BardaRash structure led to formation of the bend in Maqloub–BardaRash structure, and Rhombus outline with wavy pattern to the deformation front of the present structure (Koyi et al. 2016) (Figs. 1 and 3).

Analyzed data suggest that each segment has its own structural geometrical elements. The sense of a normal asymmetry at the Maqloub segment changed to the sense of a reverse asymmetry at the BardaRash segment. In comparison with Maleki (2015), the studied strike-slip fault might be rooted from basement. Maleki (2015) recorded anticlinal segment inversion in the Phanerozoic strata, in which segmented by a traverse basement fault become asymmetric, and sense of the asymmetry would reverse where the anticline cuts by basement fault.

Also, right-lateral strike-slip fault was observed in the Maqloub structure at the northwestern plunge. This fault is oblique to the general trend of the Maqloub anticline and resulted in shifting and/or deflection of the hinge line. This denotes to that right-lateral strike-slip fault developed during late stages of folding.

Fault-related fold model of the studied structure

The geometry of balanced cross section is a useful tool for establishing a plausible model for structures. Various models will be discussed based on the analysis of fold geometry and kinematic of evolution of thrust-related fold. The fault bend fold model for both segments of the present structure is excluded due to the absence of the upper flat. Additionally, in the fault bend fold model, the geometry of the anticline-syncline pair should reflect the shape of the bended fault (i.e., the relatively long flat and short ramp). This is also in disagreement with the present cross-sectional geometry. Moreover, the presence of the warped beds in the footwall of the major thrust rather than in the horizontal beds is an indicator that these wrapped beds were undergone folding processes prior to cutting by the thrust ramp.

The detachment folds are growing as a consequence of folding of the rock units over a basal ductile detachment. Subsequently, with progressive folding and tightening, the thrust ramp propagates through the frontlimb and backlimb

Table 1 Different shortening values that calculated at the cross section A-A⁻ (Maqloub segment) and section B-B⁻ (BardaraRash segment)

Formation/Age	Original length Km	Deformed length Km	Thrust-related Shortening Km	Fold-related Shortening Km	Total shortening Km	Shortening in percent	Average Shortening percent	Structural segment
Top Fatha (L. Fars)/ Middle Miocene	7.07	6.08	0.156	0.834	0.99	14%	11.2%	Maqloub segment
Top Pila Spi/Middle-Late Eocene	7.04	6.08	0.146	0.814	0.96	13.14%		
Top Gercus/Middle Eocene	6.90	6.08	0.138	0.682	0.82	11.88%		
Top Bekhma/Late Campanian	6.86	6.08	0.164	0.616	0.78	11.37%		
Top Qamchuqa/Early Cretaceous	6.92	6.08	0.172	0.668	0.84	12.14%		
Top Najmah/Late Jurassic	6.79	6.08	0.198	0.512	0.71	10.46%		
Top Alan/Early Jurassic	6.72	6.08	0.346	0.294	0.64	9.5%		
Top Butmah/Early Jurassic	6.71	6.08	0.262	0.368	0.63	9.39%		
Top Baluti/Late Triassic	6.69	6.08	0.272	0.338	0.61	9.11%		
Top Kurra chine/Late Triassic	6.66	6.08	0.268	0.312	0.58	8.17%		
Top Injana(U.Fars)/Late Miocene	11.99	10.84	0.528	0.622	1.15	9.59%	9.67%	Bardara Rash segment
Top Fatha (L. Fars)/ Middle Miocene	12.03	10.84	0.544	0.646	1.19	9.89%		
Top Pila Spi/Middle-Late Eocene	11.95	10.84	0.562	0.548	1.11	9.29%		
Top Khurmala/Early Eocene	11.89	10.84	0.576	0.474	1.05	8.83%		
Top Bekhma/Late Campanian	11.99	10.84	0.598	0.552	1.15	9.59%		
Top Qamchuqa/Early Cretaceous	11.99	10.84	0.616	0.534	1.15	9.59%		
Top Najmah/Late Jurassic	12.09	10.84	0.632	0.618	1.25	10.34%		
Top Alan/Early Jurassic	12.01	10.84	0.638	0.532	1.17	9.74%		
Top Butmah/Early Jurassic	12.03	10.84	0.658	0.532	1.19	9.89%		
Top Baluti/Late Triassic	11.99	10.84	0.662	0.488	1.15	9.59%		
Top Kurra chine/Late Triassic	12.04	10.84	0.668	0.532	1.2	9.97%		

of the anticline. These changes in the detachment fold geometry lead to complex anticlinal geometry and may result in misinterpretation with a fault propagation fold (Mitra and Namson 1989; Mitra 2002). In order to constrain the fold model of the Maqloub segment whether it is a detachment fold or a fault propagation fold, several characters were taken into consideration. First, both disharmonic detachment and lift-off detachment fold models are mostly symmetrical fold (Mitra and Namson 1989; Mitra 2003). The present anticline (Maqloub segment) is asymmetrical. Second, the geometry of the flat-topped detachment fold is a wide hinge region and with a steep to vertical orientation than at both flanks (Mitra and Namson 1989). The anticlinal geometry of the Maqloub segment shows somewhat broad hinge zone with shorter steeper forelimb than their backlimb. These structural properties of the aforementioned detachment models are different from structural geometry of the Maqloub segment anticline. Therefore, the detachment fold model is excluded. Alternatively, fault propagation fold model appears to be more reasonable interpretation for the Maqloub segment anticline due to the following evidences. First, the Maqloub thrust-related anticline was characterized by the existence of emerged ramps without any connection with the upper flat which seems to be absent. Second, the Maqloub structure is a very asymmetrical anticline. Third, the progressive increase of displacement was downsection along the Maqloub faults (MT1 and MT2). Fourth, increase in the thrust displacement downdip coincides with the tightening of the Maqloub anticline downsection. Fifth, the Maqloub thrust fault cuts through the hinge surface of the adjacent Merge syncline.

Based on the balanced cross section B-B⁻ (Fig. 13), the BardaRash segment anticline seems to be representative of a faulted detachment fold model. According to Mitra (2002), in the faulted detachment fold model, the fault ramps propagate through rotated panels on both flanks. This model is apparently similar to the fault propagation fold, but it is a product of the transition in deformation behavior from detachment folding to progressive fault propagation folding (Mitra 2002, 2003). In this sense, the following discussion concerns characteristic features of faulted detachment fold (Mitra 2002), which are more compatible with BardaRash fold geometries rather than fault propagation fold owing to the following. First, the current sectional geometry of the BardaRash segment fold is generally more open and rounded in comparison to the Maqloub fault propagation fold. Second, along part of the back thrust BT1 (Fig. 13) in the BardaRash anticline, the displacement distribution exhibits a nonuniform variation, which possibly related to the behavior of the fault propagation. This nonuniform variation somewhat increases or decreases downsection, or may remain constant within the Upper Triassic and Jurassic stratigraphic units. However, the displacement pattern in the Maqloub fault propagation fold has a uniform variation and decreases progressively upward along

both MT2 and MT1. Third, in the Maqloub fault propagation fold, the backlimb dips at an angle that is not steeper than the fault ramp dip angle. In the BardaRash faulted detachment fold, a domain on the backlimb dips by an amount greater than the ramp dip. Fourth, adjoining syncline across BardaRash faulted detachment has sunk below the original position in comparison with the Maqloub fault propagation fold. This sink is generally agreed to the faulted detachment folds' model of Mitra (2002). Fifth, the structural geometries of the balanced cross section and its restored counterpart are indicating smaller variations in anticlinal length of the BardaRash segment in comparison to the Maqloub fault propagation fold.

Kinematic of the Maqloub–BardaRash thrust anticline

The oldest exposed folded stratigraphic units over the present level of the ramp thrust at the Maqloub thrust propagation fold are Kolosh and Khurmala Formations. This implies that these rock units folded prior to the thrust ramp breaking through them (Mitra 1990; Suppe and Medwedeff 1990). The less competent Campanian-Maastrichtian Shiranish and Middle Eocene Gercus Formation successions possess significant anisotropic mechanical behavior. These rock units are possibly affected by minor thinning on the forelimb of the Maqloub segment anticline. The thickness changes occur in the frontlimb within the unfaulted folded rock units, and when the thrust ramp breaks through the folded succession, the thickness variations ceases (e.g., Jamison 1987; Mitra 1990; Suppe and Medwedeff 1990; Chester and Chester 1990). Based on this mechanism, fold amplification and hinge zone tightening with partial overturning might have taken place in the frontlimb of the Maqloub anticline before the propagation of the thrust ramps through the Shiranish and Gercus Formation succession. The competent successions that underlain Shiranish Formation (i.e., Bekhme Formation) and overlain Gercus Formation (Pila Spi Formation) are considerably maintained their thicknesses in all units. These competent units have deformed primarily by flexural slip mechanism (layer parallel shear), reflecting the parallel fold style: class B of Ramsay (1967). Subsequently, in the next stage of progressive deformation, the major thrust ramps cut the whole folded rock units with a footwall shortcut and a foreland vergency propagating from the major thrust ramp. During this stage rotation and modification in the geometry of Maqloub thrust propagation, anticline occurred through ramping within both flanks. Hence, overall, the Maqloub structure represents a synclinal breakthrough transported thrust propagation fold.

In contrast, the BardaRash faulted detachment fold is possibly developed above a horizontal to subhorizontal detachment surface that mostly lies within the less competent ductile evaporites of lower Triassic units with low frictional

resistance. In the case of the BardaRash faulted detachment fold, both Dusara and Amyan synclines initiated at the same time of the initiation of the BardaRash symmetric anticline. Accordingly, the interlimb angle of the BardaRash anticline decreased with the progressive shortening (Mitra 2002). Furthermore, there is a minor increase in the BardaRash anticlinal area and in turn a minor decrease in the adjoining synclinal area which is raised from material migration (Mitra 2002). The evidence of this migration can be detected at the crestal domains of BardaRash structure within Late Miocene Injana (Upper Fars) Formation, in which smaller-scale thrust fault propagated with displacement ~ 30 m (Fig. 11). This thrust fault is possibly developed as a response to migration and squeezing of material at crestal region, and it regarded to be a fold-accommodation thrust. During this stage, both flanks of the BardaRash anticline had mostly same dip and length. Thereby, the growth of the thrust ramps BT1 and BT2 of the steep flank domains took place at same time on both flanks (Mitra 2002). Later, the major forethrust (BT2) linked with the lower detachment surface and governed the subsequent asymmetric propagation of the BardaRash anticline, while the back thrust BT1 ended against the major fault BT2 (Mitra 2002). During further propagation of the BardaRash symmetric anticline, deformation relatively concentrated on the backlimb, and led to alteration of the symmetrical geometry to a slightly reverse asymmetry anticline (Mitra 2002).

The thickness variation in the Mukdadiya and Injana Formations across both limbs of the BardaRash and Maqloub segments, respectively, may denote that these variations in thickness suggest that the structures were active during deposition of the formations. This interpretation is in good accordance with Koshnaw et al. (2016). They regarded syntectonic growth strata of the Mukdadiya Formation as indicative of synkinematic deposition at the Kirkuk frontal fault structure. It has been considered that the Kirkuk frontal thrust was active during deposition of the Mukdadiya Formation.

Thin- and thick-skinned tectonics

In general, there are two scenarios concerning the tectonic style of the ZFTB, which are thin- and thick-skinned tectonics. The thin-skinned tectonic model was characterized by noninvolvement of the Precambrian basement structures in the younger Phanerozoic stratigraphic column deformation. The ZFTB is a NW-SE trending mountain belt that was evolved from the Oligocene-Pleistocene Zagros orogeny (Fard et al. 2006). The Zagros orogeny caused contraction and deformation of the overlying Phanerozoic sedimentary covers without structural contribution of the underlying crystalline basement (Davis and Engelder 1985; Blanc et al. 2003; Sepehr et al. 2006). In contrast, the thick-skinned deformation style includes involvement of the basement faults through inversion (i.e., reverse-reactivation) of sets of the preexisting faults, as

well as basement segmentation into separate blocks. These basement faults and blocks played essential role in the shortening and deformation of the younger sedimentary succession (Stoneley 1981; Edgell 1996; Bahroudi and Talbot 2003; Sherhati and Letouzy 2004). Some researchers deemed coexistence of both thin-skinned tectonics and involvement of basement in the shortening of Zagros belt. For instance, Molinaro et al. (2005) and Mouthereau (2007) regarded the southeastern part of the ZFTB subjected to a Miocene-Pliocene thin-skinned shortening and to a Pliocene-Recent thick-skinned tectonics. On the other hand, Molnar and Tapponnier (1975) highlighted the influence of the strike-slip fault on cutting and rotation of anticlinal hinge traces across the Himalayas fold thrust belt. These faults are oriented oblique to the regional trend of the Himalayas belt and originated from underlying basement (Baker et al. 1993); therefore, these basement faults are contributing to the deformation of the belt as well. Whereas, Islam and Shinjo (2010) deduced that thrust faults with strike-slip component are prevalent through deeper crustal horizon within ZFTB and at depth exceeded 10 km in ZFTB.

Based on the line length balanced cross sections from this study, the segments of the Maqloub–BardaRash structure reflect their particular model of fold evolution. From the cross-section A-A⁻ geometries (Fig. 12), the Maqloub segment structural propagation is mostly affected by a thrust fault that rooted from basement and led to slipping of the basement. Thus, the Maqloub segment was interpreted as a thick-skinned deformation style. This interpretation can be supported by existence of a frontal thrust fault with strike-slip component within the Maqloub structure (Fig. 3). Moreover, the elevation values of the structural relief (i.e., uplifting) across the Maqloub and BardaRash segments (A-A⁻ and B-B⁻ sections) are exhibiting remarkable different results. This can be calculated by comparison between a specified regional marker horizon at the hinges of the synclines across A-A⁻ and B-B⁻ sections. For instance, by taking top of Fatha (Lower Fars) Formation, it reveals that the difference in uplifting across section A-A⁻ is greater than section B-B⁻ and estimated to be 1700 m. However, here, we must take into consideration the effect of sinking of syncline according to Mitra (2002). Sinking syncline occurs only across the section B-B⁻ (BardaRash faulted detachment fold), which led to increase of the differential uplifting values between the two segments. The amount of the syncline sinking is relatively small; it is assumed to be between 100 and 300 m. Thus, the rest of the uplifting value is more than 1400 m. In the light of basic principles of the section balancing technique, the regional marker horizon has had the same original regional level prior to shortening (Woodward et al. 1989). As noted, the calculated shortening across Maqloub segment is small relatively, but it is in agreement with other measurements of shortening across the ZFTB that estimated to be ranged 10–15% (McQuarrie

2004; Emami et al. 2010; Verges et al. 2011; Frehner et al. 2012; Omar and Syan 2016; Koshnaw et al. 2016). Moreover, few workers pointed to the necessity of basement involved shortening for balancing the differential uplift between abutting synclines across northwestern ZFTB in Iran (Blanc et al. 2003; Sherkati and Letouzey 2004). By taking the aforementioned information into account, the small value (11.2%) of the estimated average shortening is impossible to be responsible for creating the current uplift of Maqloub segment, particularly with absence of a very thick incompetent weak sequence (i.e., mobile horizon). Accordingly, the extra elevation along Maqloub segment occurs solely via involvement of basement thrust faulting which necessitated to preserve the present topographic reliefs. Also, seismic activity that was documented in the Iraqi Kurdistan Zagros belt back up this interpretation, so that the deformation of the basement drive by thrust faults and basement segmentation (basement blocks) within the upper part of Earth's crust (Jassim and Goff 2006). The strongest evidence comes from a seismic line that passes through northwestern plunge of the Maqloub segment. In this reflection seismic image, it demonstrates that the southwestern frontal thrust was penetrated most rock units of the Lower Paleozoic sequence by high angle ($\sim 60^\circ$). This possibly suggests that southwestern frontal thrust at Maqloub segment is not detached and flattened within Phanerozoic stratigraphic units, but is rather rooted within the Precambrian basement. In contrast, from the section B-B' geometry (Fig. 13), it was observed that BardaRash segment floored and decoupled within detachment of the incompetent evaporite layers of the lower Triassic Kurra Chine Formation without involving basement fault. Therefore, BardaRash segment can be a representative of a thin-skinned style of deformation.

Conclusions

The Maqloub–BardaRash structure is deemed to be a special and a unique anticline in the northwestern of ZFTB within Iraqi Kurdistan that exhibits two unlike geometrical models along their strike. The Maqloub segment is interpreted as a thrust propagation anticline, whereas the BardaRash segment is a faulted detachment fold.

The structural characteristics of the Maqloub–BardaRash anticline change along strike from Maqloub normal asymmetrical anticline to BardaRash reverse asymmetrical anticline.

The transverse left-lateral strike-slip fault led to an abrupt deviation and rotation of the anticlinal hinge of Maqloub–BardaRash structure by $\sim 20^\circ$ and show persistence to the adjacent structures. This strike-slip fault is regarded to be a basement fault.

The longitudinal basement thrust fault involved in accommodating the differential uplifting along the strike of Maqloub–

BardaRash structure. Consequently, the Maqloub segment has been uplifted by ~ 1.4 km compared to the BardaRash segment.

It is interpreted that each segment has a different detachment level from another. Thus, along the studied structure, the tectonic style changed from thin skin deformation at BardaRash segment to basement involved, thick skin deformation within Maqloub part.

It seems that via overall structural geometries, understanding of the two different models of the fault-related deformation along the individual Maqloub–BardaRash anticline will possibly help to identify more accurate well location of the crestal reservoir.

The intensity of deformation along the Maqloub structure that lies within the LFZ is greater than the nearby folds in the HFZ, such as the Pirmam anticline in the less deformed (outer) part of the HFZ (Fig. 1). Hence, we suggest that in the future proposed tectonic division of Zagros belt in Iraqi Kurdistan, the subsurface structural portioning should be taken into account rather than just the surface geological features.

References

- Agard P, Omrani J, Jolivet L, Mouthereau F (2005) Convergence history across Zagros (Iran): constraints from collisional and earlier deformation. *Int J Earth Sci* 94:401–419. <https://doi.org/10.1007/s00531-005-0481-4>
- Aqrabi AAM, Goff JC, Horbury AD, Sadooni FN (2010) The petroleum geology of Iraq. Statoil Scientific Press 424p
- Awdal A, Healy D, Alsop GI (2016) Fracture patterns and petrophysical properties of carbonates undergoing regional folding: a case study from Kurdistan Iraq. *Mar Pet Geol* 71:149–167
- Bahroudi A, Talbot CJ (2003) The configuration of the basement beneath the Zagros Basin. *J Pet Geol* 26:257–282
- Baker C, Jackson J, Priestley K (1993) Earthquakes on the Kazerun line in the Zagros Mountains of Iran: strike-slip faulting within a fold-and-thrust belt. *Geophys J Int* 115:41–61
- Blanc EJP, Allen MB, Inger S, Hassani H (2003) Structural style in Zagros simple folded zone, Iran. *J Geol Soc* 160(3):401–412. <https://doi.org/10.1144/0016-764902-110>
- Bretis B, Bartl N, Grasemann B (2011) Lateral fold growth and linkage in the Zagros fold and thrust belt (Kurdistan, NE Iraq). *Basin Res* 23: 615–630
- Burberry CM (2015) The effect of basement fault reactivation on the Triassic—recent geology of Kurdistan, North Iraq. *J Pet Geol* 38(1):37–58
- Chester JS, Chester FM (1990) Fault-propagation folds above thrusts with constant dip. *J Struct Geol* 12:903–910
- Cotton JT, Koyi HA (2000) Modeling of thrust fronts above ductile and frictional detachment: application to structures in the Salt Range and Potwar Plateau, Pakistan. *Geol Soc Am Bull* 112:351–363
- Csontos L, Sasvári A, Pocsai T, Kósa L, Salaa A, Ali A (2012) Structural evolution of the northwestern Zagros, Kurdistan Region, Iraq: implications on oil migration. *GeoArabia* 17(2):81–116
- Dahlstrom CD (1969) Balanced cross-section. *Can J Earth Sci* 6:743–757
- Davis DM, Engelder T (1985) The role of salt in fold and thrust belts. *Tectonophysics* 119:67–88

- Dobson JMM (1991) The dynamics of foreland fold-and-thrust belts, southern Canadian Rocky Mountains, SW Alberta, Canada. Unpublished PhD thesis, Royal Holloway, University of London, 316p
- Edgell HS (1996) Salt tectonism in the Persian Gulf basin. In: Alsop GI, Blundell DJ, Davison I (Eds), Salt tectonic, London, pp129–151
- Ellis MA, Dunlap WJ (1988) Distribution variation along thrust faults: implications for the development of large faults. *J Struct Geol* 10: 183–192
- Emami H, Verges J, Nalpas T, Gillespie P, Sharp I, Karpuz R, Blanc EJP, Goodarzi MGH (2010) Structure of the mountain front flexure along the Anaran anticline in the Pusht-e Kuh Arc (NW Zagros, Iran): insights from sand box models. In Tectonic and stratigraphic evolution of Zagros and Makran during the Mesozoic-Cenozoic (eds. Leturmy P & Robin C), Geological Society, London, Special Publication, No. 330, pp. 155–178
- English JM, Lunn GA, Ferreira L, Yacu G (2015) Geologic evolution of the Iraqi Zagros, and its influence on the distribution of hydrocarbons in the Kurdistan region. *AAPG Bull* 99(2):231–272
- Fard IA, Braathen A, Mokhtari M, Alavi SA (2006) Interaction of the Zagros fold-thrust belt and the Arabian-type, deep-seated folds in the Abadan Plain and the Dezful Embayment, SW Iran. *Pet. Geosci* 12:347–362
- Frehner M, Reif D, Grasemann B (2012) Mechanical versus kinematical shortening reconstructions of the Zagros High Folded Zone (Kurdistan region of Iraq). *Tectonics* 31:TC3002
- Golonka J (2004) Plate tectonic evolution of the southern margin of Eurasia in the Mesozoic and Cenozoic. *Tectonophysics* 381: 235–273
- Groshong RH (2006) 3-D structural geology. Springer-Verlag, Berlin, p. 324
- Hessami K, Koyi HA, Talbot CJ, Tabasi H, Shabaniyan E (2001) Progressive unconformities within an evolving foreland fold-thrust belt Zagros Mountains. *J Geol Soc, Lond* 158:969–981
- Horton BK, Yin A, Purlin MS, Zhou J, Wang J (2002) Paleocene-Eocene syncontractual sedimentation in narrow, lacustrine-dominated basins of east-central Tibet. *Geol. Soc. Am. Bull.*, v.114, pp.771–786.
- Howard JH (1993) Restoration of cross-sections through unfaulted, variably strained strata. *J Struct Geol* 9:207–219
- Islam MS, Shinjo R (2010) Nontectonic stress field and deformation pattern within the Zagros and its adjoining area: an approach from finite element modeling. *J Geol Min Res*, v. 2(7):170–182
- Jabbour M, Dhont D, Hervouet Y, Deroin J (2012) Geometry and Kinematics of fault-propagation folds with variable interlimb angle. *J Struct Geol*. <https://doi.org/10.1016/j.jsg.2012.05.002>
- Jamison WR (1987) Geometric analysis of fold development in over thrust terranes. *J Struct Geol* 9:207–209
- Jassim SZ, Goff JC (2006) Geology of Iraq. Dolin, Prague Moravian Museum, Brno, Zech.Repub.341p.
- Kent N (2010) Structure of the Kirkuk Embayment, northern Iraq: foreland structures or Zagros Fold Belt structures. *GeoArabia* 15(4): 147–188
- Koshnaw RI, Horton BK, Stockli DF, Barber DE, Tamar-Agha MY, Kendall JJ (2016) Neogene shortening and exhumation of the Zagros fold-thrust belt and foreland basin in the Kurdistan region of northern Iraq *Tectonophysics*. <https://doi.org/10.1016/j.tecto.2016.11.016>
- Koyi H, Nilfouroushan FF, Hessami K (2016) Modelling role of basement block rotation and strike-slip faulting on structural pattern in cover units of fold-and-thrust belts. *Geol.Mag* 153(5/6):827–844. <https://doi.org/10.1017/S0016756816000595>
- Maleki Z, (2015) The unique folding style in the Zagros simply folded belt, the Kuh-e Qazi anticline, south Iran. *J Geol*5, <https://doi.org/10.4236/ojg.2015.57047>.
- Masaferro JL, Poblet J, Blunes M, Eberli GP (2002) Episodic folding inferred from syntectonic carbonate sedimentation: the Santaren anticline, Bahamas foreland. In: Marzo M, Munoz JA, Vergus J.(Eds.), *Sedimentary geology*, v. 146, p.11–24.
- McClay KR (2004) Thrust tectonics and hydrocarbon systems: introduction, in McClay KR, ed., *Thrust tectonics and hydrocarbon systems*. AAPG Memoir,82, pp. ix–xx.
- McConnel DA, Kattenhorn SA, Benner L (1997) Distribution of fault slip in outcrop-scale fault-related folds, Appalachian Mountains. *J Struct Geol* 19:257–267
- McQuarrie N (2004) Crustal scale geometry of the Zagros fold-thrust belt, Iran. *J Struct Geol* 26:519–535
- Mitra S (1986) Duplex structures and imbricate thrust systems: geometry, structural position and hydrocarbon potential. *AAPG. Bull.* 70: 1087–1112
- Mitra S (1990) Fault-propagation folds: geometry, kinematic evolution, and hydrocarbon traps. *AAPG. Bull.* 74:921–945
- Mitra S (1992) Balanced structural interpretations in fold and thrust belts. In: Mitra S, Fisher GW (eds) *Structural geology of fold and thrust belts*. Johns Hopkins University Press, Baltimore, Maryland, pp 53–77
- Mitra S (2002) Structural geometry of faulted detachment folds. *AAPG. Bull.* 86:1673–1694
- Mitra S (2003) A unified kinematic model for evolution of detachment folds. *J Struct Geol* 25:1659–1673
- Mitra S, Namson JS (1989) Equal-area balancing. *Am J Sci* 289:563–599
- Molinario M, Guezou JC, Leturmy P, Eshraghi SA, Frizon De Lamotte D (2004) The origin of changes in structural style across the Bandar Abbas syntaxis, SE Zagros (Iran). *Mar Pet Geol*, 21, pp.735–752.
- Molinario M, Leturmy P, Guezou JC, Frizon De Lamotte D, Eshraghi SA (2005) The structure and kinematics of the south-eastern Zagros fold-thrust belt; Iran: from thin-skinned to thick-skinned tectonics. *Tectonics* 24:TC3007. <https://doi.org/10.1029/2004TC001633>
- Molnar P, Tapponnier P (1975) Cenozoic tectonics of Asia: effects of a continental collision. *Science*, 189, pp. 419–426.
- Mouthereau F, Tensi J, Bellahsen N, Lacombe O, De Boisgrollier T, Kargar S (2007) Tertiary sequence of deformation in a thin-skinned/thick-skinned collision belt: the Zagros Folded Belt (Fars, Iran). *Tectonics* 26, TC5006, <https://doi.org/10.1029/2007TC002098>.
- Omar AA, Syan SH (2016) Construction of a structural model for Harir anticline within Zagros Fold-Thrust belt, Kurdistan Iraq. *Zanco. J Pure Appl Sci* 28(6):90–105, <https://doi.org/10.21271/ZJPAS.28.6.12>
- Pennock ES, Lillie RJ, Zaman AS, Yousuf M (1989) Structural interpretation of seismic reflection data from Eastern Salt Range and Potwar Plateau, Pakistan. *AAPG. Bull.* 73:841–857
- Pirouz M, Simpson G, Bahroudi A, Azhdari A (2011) Neogene sediments and modern depositional environments of the Zagros foreland basin system. *Geol.Mag* 148(5–6):838–853
- Poblet J, Lisle RJ (2013) Kinematic evolution and structural styles of fold-and-thrust belts. *Geol Soc, Lond. Spec Publ* 349:1–24
- Quick JE (1991) Late Proterozoic transpression on the Nabitah fault system—implications for the assembly of Arabian Shield. *Precambrian Res* 13(3):313–334
- Ramsay JG (1967) *Folding and fracturing of rocks*. McGraw-Hill book Co., New York 568p
- Reif D, Grasemann B, Faber R (2011) Quantitative structural analysis using remote sensing data: Kurdistan, northern Iraq. *AAPG. Bull.* 95. <https://doi.org/10.1306/11151010112>
- Reif D, Decker K, Grasemann B, Peresson H (2012) Fracture patterns in the Zagros fold-and-thrust belt, Kurdistan, region of Iraq. *Tectonophysics* 576–577:46–62
- Sadooni FN (1997) Stratigraphy and petroleum prospects of Upper Jurassic carbonates in Iraq. *Pet Geosci*, v.3, pp.233–243, doi: <https://doi.org/10.1144/petgeo.3.3.233>.

- Sepehr M, Cosgrove J, Moieni M (2006) The impact of cover rock rheology on the style of folding in the Zagros fold-thrust belt. *Tectonophysics*, 427(1), pp.265–281.
- Sharland PR, Archer R, Casey DM, Davies RB, Hall SH, Heward AP, Horbury AD, Simmons MD (2001) Arabian plate sequence stratigraphy. *GeoArabia*, Special Publication 2, Gulf Petro Link, Manama, 371p.
- Shaw J H, Connors C, Suppe J (2005) Seismic interpretation of contractional fault-related folds. *An AAPG seismic atlas: AAPG Studies in Geology*, 53, 156 p.
- Sherkati SM, Letouzey J (2004) Variation of structural style and basin evolution in the central Zagros (Izeh zone and Dezful Embayment), Iran. *Mar Pet Geol* 21(5):535–554
- Sissakian VK (2013) Geological evolution of the Iraqi Mesopotamia Foredeep, inner platform and near surroundings of the Arabian Plate. *J Asia Earth Sci* 72:152–163
- Stoneley R (1981) The geology of the Kuh-e Dalneshin area of southern Iran, and its bearing on the evolution of southern Tethys. *J Geol Soc, Lond* 138:509–526
- Sun J, Zhang Z (2009) Syntectonic growth strata and implications for late Cenozoic tectonic uplift in the northern Tian Shan, China. *Tectonophysics* 463(1):60–63
- Suppe J, Medwedeff DA (1990) Geometry and kinematics of fault-propagation folding. *Eclo. Geol. Helv.*, v. 83, pp. 409–454.
- Talbot CJ, Alavi M (1996) The past of a future syntaxis across the Zagros. In: Alsop GI, Blundell DJ, Davison I (Eds.), *Salt Tectonics*, v. 100. Geological Society, London, Special Publications, pp. 89–109.
- Tavani S, Storti F, Salvini F (2006) Double-edge fault-propagation folding: geometry and kinematics. *J Struct Geol* 28:19–35
- Van Bellen R C , Dunnigton H V, Wetzel R and Morton D (1959) *Lexique stratigraphique international, Asie, Fascicule 10a, Iraq*. Paris, 333 p
- Verges J, Goodarzi MGH, Emami H, Karpuz R, Efstathiou J, Gillespie P (2011) Multiple detachment folding in Pusht-e-Kuh arc, Zagros: role of mechanical stratigraphy, in McClay K, Shaw JH, Suppe J eds., *Thrust fault-related folding: AAPG Memoir*94, pp.69–94.
- Woodward NB, Boyer SE, Suppe J (1985) An outline of balanced cross-sections. University of Tennessee, Department of Geological Sciences Studies in geology. 11,2 ed., 173p.
- Woodward NB, Boyer SE, Suppe J (1989) Balanced geological cross-sections: an essential technique in geological research and exploration. *Short Course in Geology*, Washington, DC. Am Geophys Union 6:132p